Proceedings of GT2007:
ASME Turbo Expo 2007: Power for Land, Sea and Air
May 14-17, 2007, Montreal, Canada

GT2007-27302

APPLICATION OF MADYN 2000 TO ROTORDYNAMIC PROBLEMS OF INDUSTRIAL MACHINERY

Joachim Schmied
DELTA JS, Switzerland

Marco Perucchi
DELTA JS, Switzerland

Jean-Claude Pradetto
DELTA JS, Switzerland

ABSTRACT

The special requirements of rotordynamics engineering are illustrated by means of different examples of turbomachines. The differences between the properties of magnetic bearings and the more common fluid film bearings are pointed out in the examples of two turbocompressors. The importance of the bearing support properties are shown for a turbine generator train. The impact of seal forces are demonstrated for the turbocompressor supported on fluid film bearings. Two of the considered seals are honeycomb seals with frequency dependent characteristics. The consequences of the coupling of lateral and torsional vibrations in gears are illustrated for a gear compressor with three pinions. All examples have a practical background from troubleshooting and engineering work although they do not exactly correspond to real cases.

INTRODUCTION

Rotors are structures with special properties due to their rotation (causing e.g. the gyroscopic effect), due to their bearings (fluid film bearings, magnetic bearings) and in many cases due to surrounding fluids (seal forces). Therefore rotordynamics requires special engineering tools although the structural properties of the rotors and their supports could well be modeled by any general finite element program.

Tools for rotordynamics and bearings have been developed for many years. Pioneers in this area are Lund [1], Nordmann [2], Nelson [3],[5] and Gasch [4]. Nordmann, Nelson and Gasch introduced the finite element method to rotordynamics. Lund developed the basics for fluid film bearings, which were further refined by many researchers such as for example Glienicke [6].

The recent development of magnetic bearings, which are now more and more introduced in industrial applications of turbomachines, required an extension of existing rotordynamic tools to model the specific characteristics of this bearing type and the controllers (see [7]).

The differences in the rotordynamic behavior of rotors supported on classic tilting pad fluid film bearings and magnetic bearings are illustrated in two turbocompressor examples.

The impact of the bearing support behavior is shown for the example of a turbine generator train supported on fluid film bearings.

The interaction of fluid forces and seals has been the topic of research for many years, which is still going on. Well known researchers in this area are Nordmann [8] and Childs [9]. A few years ago fluid forces were mainly modeled as stiffness and damping coefficients. Recently it is more and more recognized thanks to more sophisticated analysis tools and measurements, that this approach is too restrictive. Honeycomb seals for example can have more complex frequency dependent characteristics (see [10],[11]). Still, the rotordynamic tools for the consideration of fluid forces are not as established as for fluid film bearings and strongly simplified engineering approaches are frequently used, for example the procedure described in API [12] as stability level I analysis. In this paper an approach which could be used as stability level II analysis, is described for a high pressure turbocompressor.

In train arrangements with gears the lateral and torsional vibrations are coupled. The influence of this coupling, which is normally not taken into account in standard analyses, is shown for a gear compressor.

All analyses in this paper were carried out with the general rotordynamic program MADYN 2000 [13]. Its mathematics of the structural modeling part is based on the proven finite element program MADYN [14]. The fluid film bearing module in MADYN 2000 goes back to the program ALP3T [15], which is the result of more than 20 years of research of the German research consortium FVV. The magnetic bearing module originates from the program MEDYN [7],[16], whose development started with the industrial application of magnetic bearings.

NOMENCLATURE

B Width of bearings
d Damping coefficient of bearings or seals
D Diameter of bearings
Damping ratio
f Frequency
k Stiffness coefficient of bearings or seals
m Pad preload of fluid film bearings

DESCRIPTION OF THE EXAMPLES

Four rotor arrangements are considered in this paper, which are described in the following chapters.

The rotor structures are modeled with finite elements according to the Timoshenko beam theory considering the shear deformation and gyroscopic effects [2],[3],[4],[5]. Each cross section can consist of superimposed cross sections with different mass and stiffness diameter as well as different material properties. The contours shown in the rotor plot represent the resulting mass diameter with the density of the basis cross section, which is normally steel.

Stiff shrunk parts on the rotor, e.g. impellers, can be modeled as rigid parts. They are represented by mass, equatorial and polar moments of inertia. In the rotor plots they are drawn as equivalent disks. In case only the mass is given and no moments of inertias they are drawn as spheres. Normally the fixation of these parts is rigid. If necessary they can also be flexibly mounted.

Several analytical results of the examples will be shown: Damped natural vibration modes at different speeds and the response to unbalance loads. The damping of natural modes will be described as damping ratio. This proved useful, since it can easily be transformed to the amplification factor in the resonance of an unbalance response. The stability can also be assessed by the damping ratio; an unstable rotor has a negative damping ratio.

1. Turbocompressor supported on fluid film bearings with seals

The model of the turbocompressor with its main data is shown in figure 1.

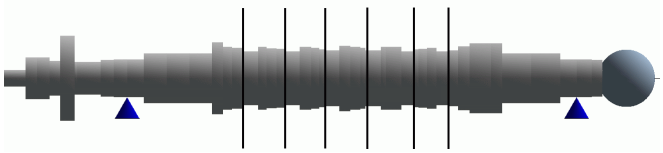

Max. speed 12’000 rpm, total rotor weight 220 kg

Figure 1. Compressor rotor on fluid film bearings

The geometry of the 5 tilting pad bearings is illustrated in figure 2. The bearing has a load on pad arrangement and all pad supports have an offset.

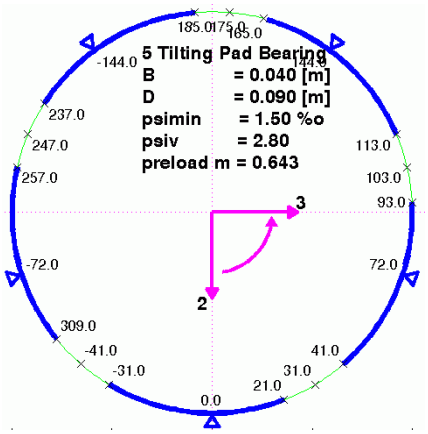

Figure 2. Radial fluid film bearing geometry

This model will also be used to demonstrate the impact of seal fluid forces. The location of the two considered labyrinth seals and honeycomb seals with the highest gas density are shown in figure 3.

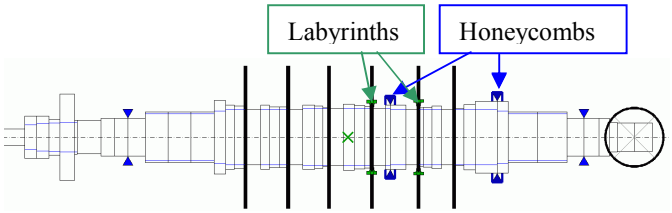

Figure 3. Seal locations on the compressor rotor

2. Turbocompressor supported on magnetic bearings

The model of the turbocompressor with its main data is shown in figure 4. The bearings are represented by their sensor and actuator. The triangle in the plot indicates the actuator location, the bar the sensor location.

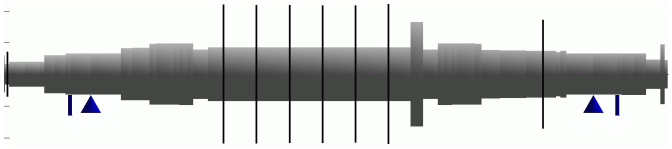

Max. speed 12’600 rpm, total rotor weight 550 kg

Figure 4. Compressor rotor on magnetic bearings

3. Turbine generator train

The model of the turbine generator train is shown in figure 5. Turbine and generator are supported on fixed pad fluid film bearings. All bearing supports are flexible with a dynamic characteristic. Each support has a resonance in horizontal and vertical direction in the range of three times operating speed. Since there is only one relevant resonance and the coupling

between the supports is negligible the supports are modeled as two separate one mass systems for the horizontal and vertical direction. In the more general case of several resonances and not negligible couplings between the supports transfer functions describing the displacement force relation could be used.

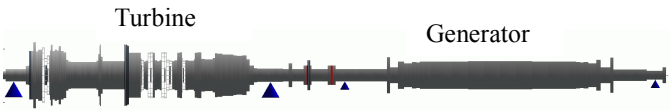

Nominal speed 3'000 rpm

Figure 5. Turbine generator shaft train

In a shaft train consisting of two rotors with two bearings each and coupled with a solid coupling the static bearing load and thus the bearing characteristics depend on the alignment, which may change due to thermal growths of supports and casings. In the present case this influence was relative small due to the high weight of the rotors and the flexibility of the solid coupling.

4. Gear compressor

The model of the gear compressor consisting of a bull gear and three pinions is shown in figure 6. All rotors are supported on fluid film bearings, the pinions on tilting pad bearings and the bull gear on cylindrical bearings.

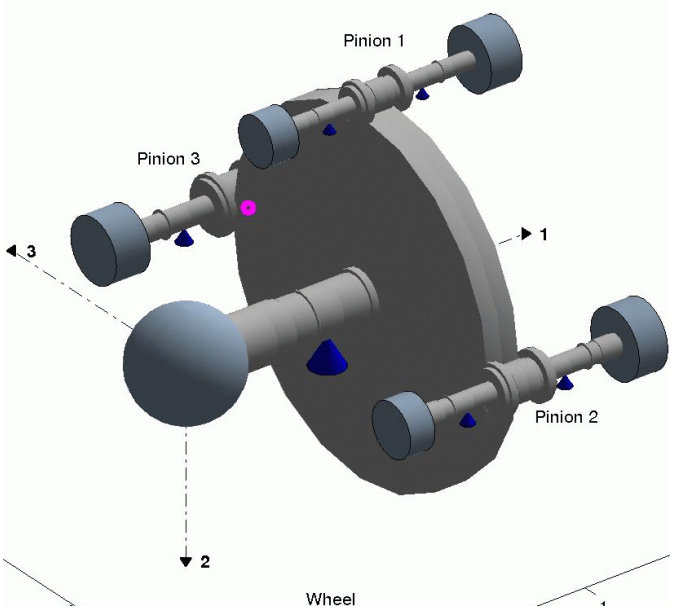

Figure 6. Gear compressor

The meshing is modeled as explained in figure 7. The spring is aligned with the tooth contact force.

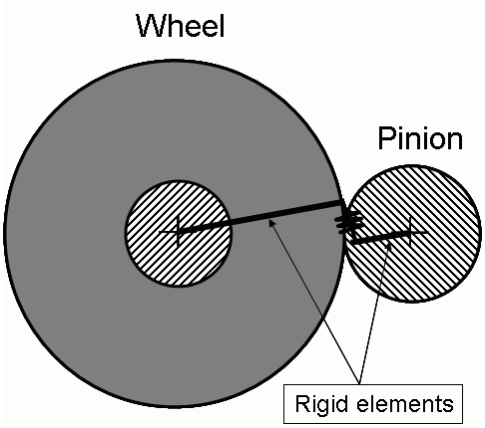

Figure 7. Modeling of the gear mesh

ROTORDYNAMIC BEHAVIOUR WITH FLUID FILM BEARINGS AND MAGNETIC BEARINGS

Rotor on fluid film bearings

The stiffness and damping coefficients of the fluid film bearings in the 2-3 coordinate system of figure 2 are shown in figure 8. The coefficients of the two bearings are almost the same. For this reason only one plot is shown. The coefficients are speed and load dependent. The load in the present case is the rotor weight.

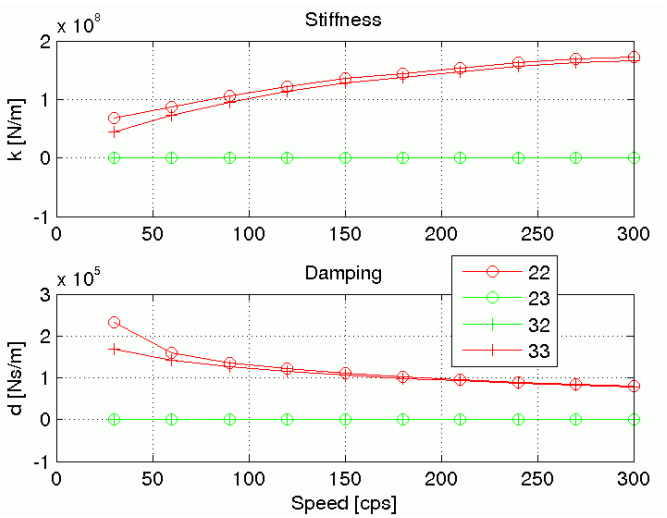

Figure 8. Stiffness and damping coefficients of the fluid film bearing (left bearing in figure 1)

The rotor speed dependent natural frequencies and damping ratios are shown in the Campbell diagram of figure 9.

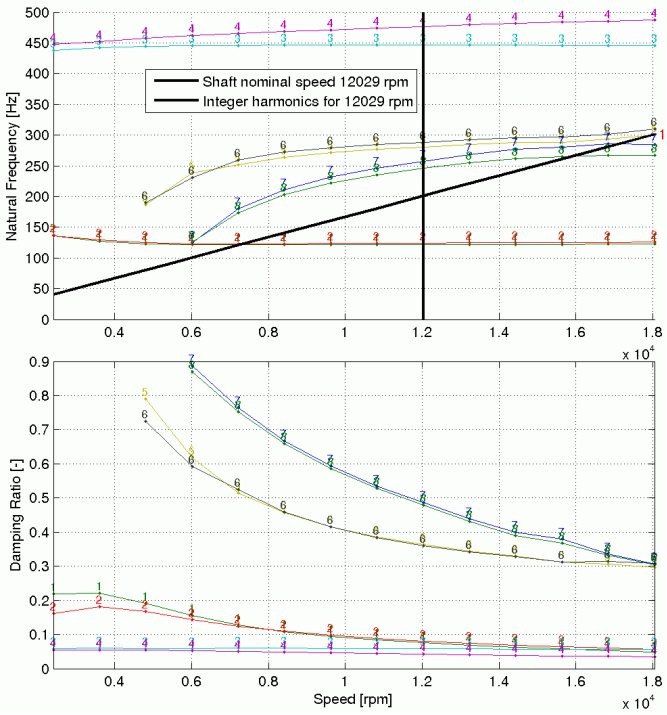

Figure 9. Campbell diagram of the compressor rotor supported on radial fluid film bearings

The mode shapes at nominal speed can be seen in figure 10. They are shown in two planes at the instant when the maximum deflection occurs. The first plane is determined by the maximum deflection and the rotor axis and the second plane is perpendicular to this plane. The first plane is indicated by the solid line in the 2-3 coordinate system and the second plane by the dashed line. The whirling direction is also indicated in the figure. A circular forward whirling orbit has the value +1 and a circular backward whirling mode the value -1. Elliptic orbits have values between 0 and +1 and -1 respectively.

The rotor runs between its first bending and its second bending mode. The separation margin from both resonances is comfortable. Between these two modes are four further modes with a huge damping around 40%. Due to their large damping they are of no practical relevance. Note, that for example API [12] considers resonances with an amplification factor of less than 2.5 corresponding to a damping ratio of more than 20% as critically damped.

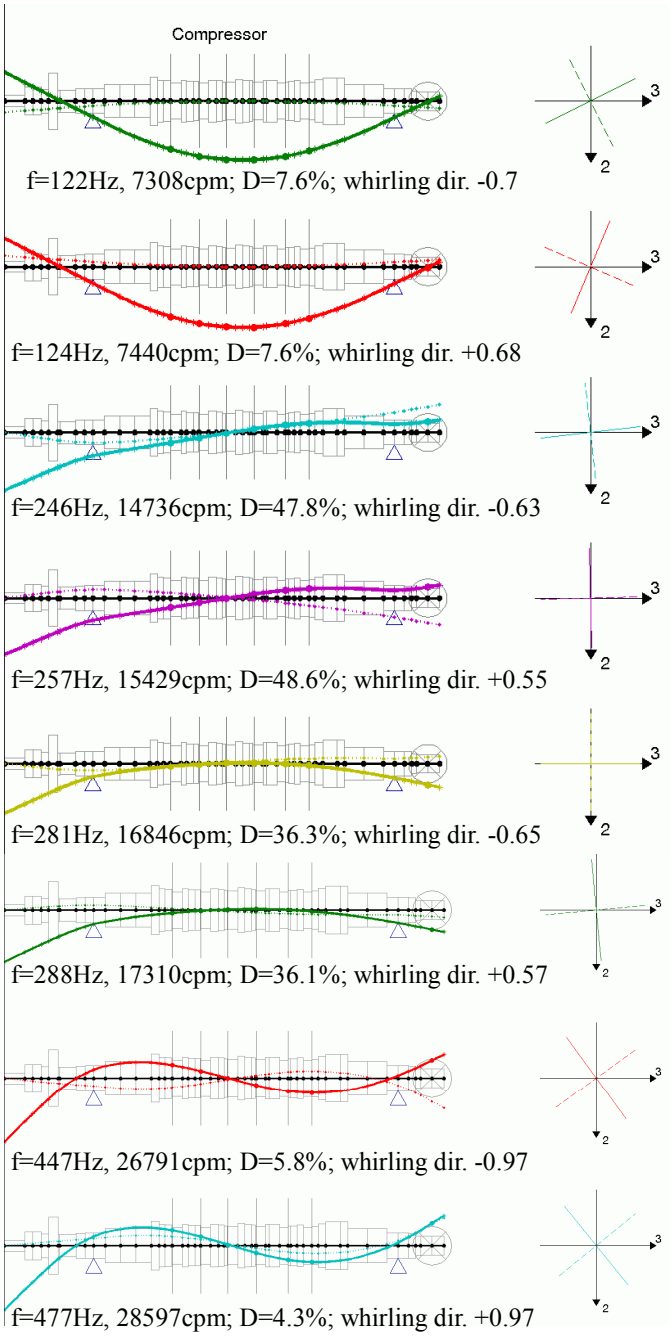

Figure 10. Natural modes at nominal speed

Rotor on magnetic bearings

In figure 11 the bearing characteristics of the magnetic bearings are shown as transfer functions. They describe the relation between the rotor displacement at the sensor and the actuator force. The hardware consisting of sensor, amplifier and actuator, the controller and digitization effects are included in the transfer functions. The eigenvalues (natural frequency and

damping ratio) of the complete system (bearing and rotor) at maximum speed are also shown in figure 11. The transfer functions are determined to a large extent by the controllers. The controllers must be designed in such a way to damp all natural modes in the speed range well and not destabilize modes at high frequencies. This must be achieved in spite of a continuous phase loss, i.e. reduction in damping, with increasing frequency due to the hardware characteristics and digitization effects. The design of a controller is for example described in [7],[16].

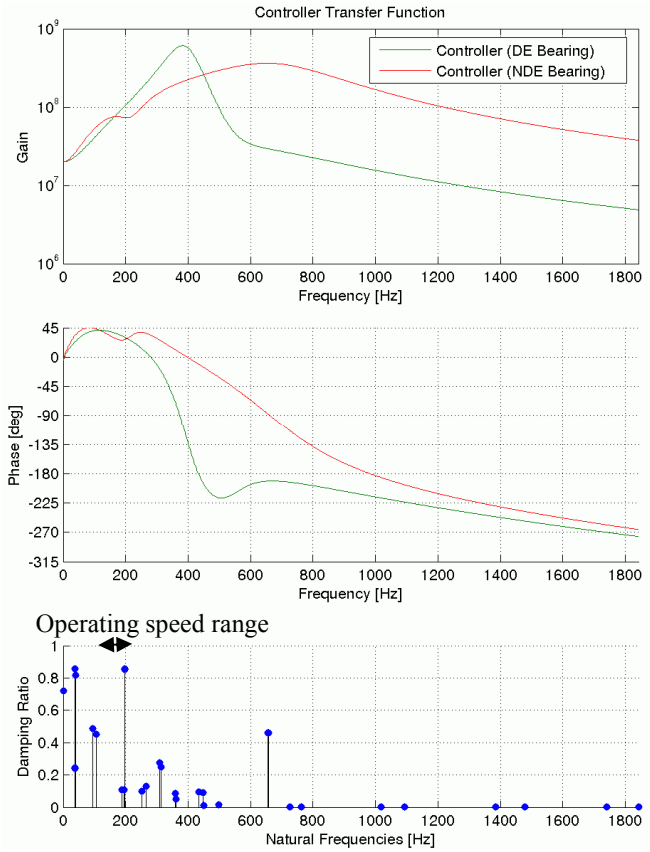

Figure 11. Magnetic bearing transfer functions and eigenvalues (damping and natural frequencies)

The mode shapes in two perpendicular planes as described for figure 10 are shown in figure 12. In case of magnetic bearings the shapes move on circles, because the bearings are completely isotropic. The indication of the direction of the maximum deflection is therefore not meaningful and omitted.

It can be seen, that in the present case all modes below maximum speed are well damped and that all modes in the higher frequency range are stable. It must be noted, that some modes marked with a capital C are not determined by the rotor but by the controller, which augments the system and causes additional modes.

Compared to the rotor on fluid film bearings the behavior is quite different. There are two pairs of forward and backward whirling well damped rigid body modes at low frequencies. They appear due to low bearing stiffness in this frequency range, which can be recognized in the transfer function in figure 11. The transfer function has a value well below 10^8 N/m. This is lower than the stiffness of the fluid film bearing of the other rotor, in spite of the fact, that the rotor for fluid film bearings is considerable smaller. The first bending modes occur at 189Hz and 194Hz, respectively. Their shape corresponds more to a free - free bending mode shape. In the present case this mode is within the speed range and the damping of 11% is not sufficient to regard it as critically damped according to API [12].

Magnetic bearings allow defining a special characteristic for frequencies synchronous to the rotor speed. This characteristic is described by a synchronous transfer function. It can be used to specially damp or filter the synchronous response. Filtering can be applied outside critical speeds to minimize the bearing force. A pure damping can be defined in the vicinity of critical speeds to minimize the response and bearing force at the same time. Thus the damping of the first bending mode in the speed range of the machine can be damped more than the 11% from the normal controller when running through it.

This feature is demonstrated for the response to an unbalance distribution as shown in figure 13. The synchronous transfer function is shown in figure 14.

The synchronous characteristic starts at 7000rpm. It corresponds to a pure damping force with a phase angle of 90°. At lower speeds the characteristic corresponds to the normal bearing transfer function as shown in figure 11.

The unbalance response with and without the synchronous transfer function is shown in figure 15 for the sensor displacements and in figure 16 for the bearing forces. The effect of the synchronous characteristic is obvious. It reduces the maximum sensor displacements in the operating speed range to 56% and the bearing forces to 31%. The shape at the maximum displacement is indicated in figure 15. It corresponds to the first bending for both cases.

A good comparison of a calculated and measured unbalance response of a rotor on magnetic bearings, which proves the validity of this type of analysis, is given in [16]. The calculated stability has been verified in many projects during the tuning process of magnetic bearing controllers (see among others [7],[16]).

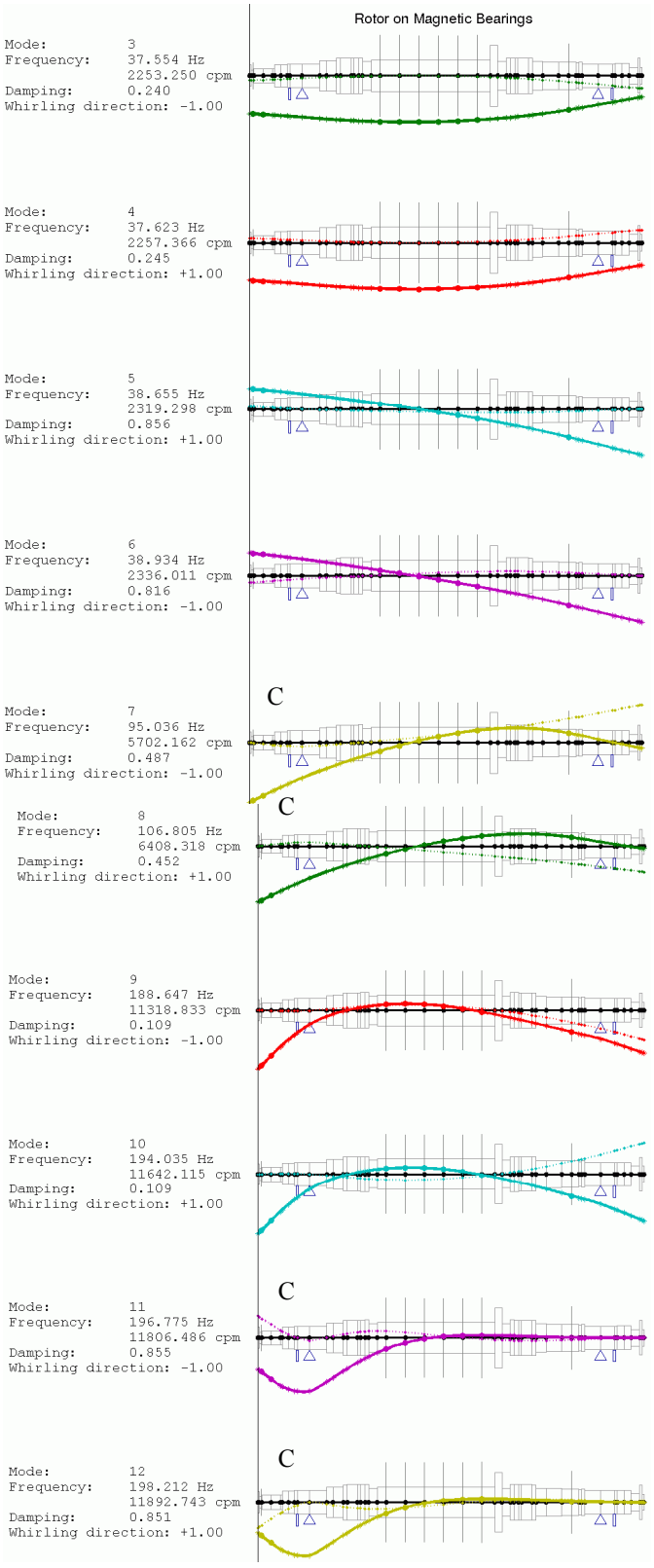

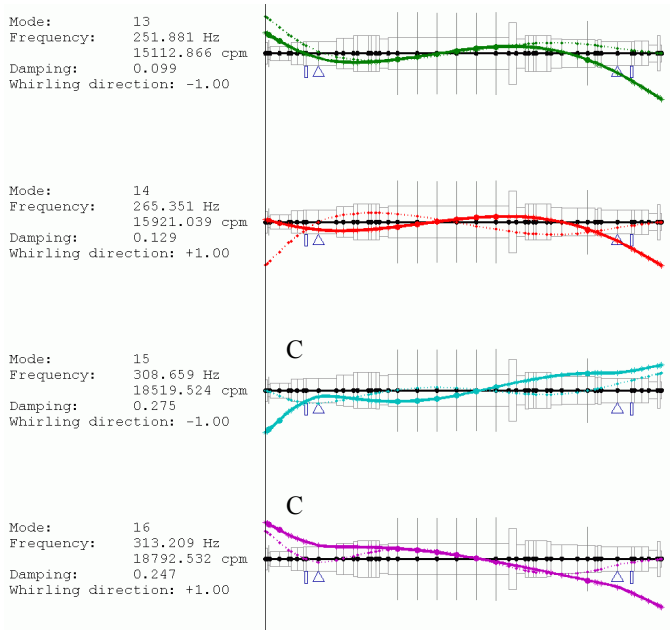

Figure 12. Natural modes nominal speed

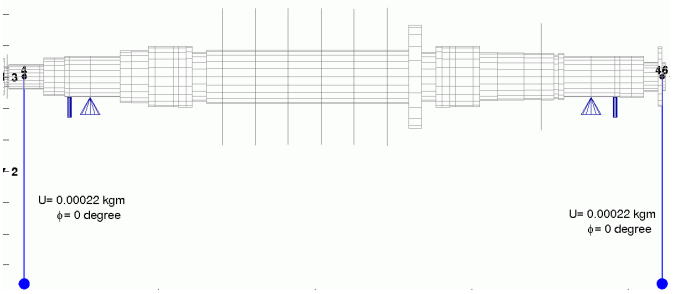

Figure 13. Unbalance distribution, magnitude corresponding to G1

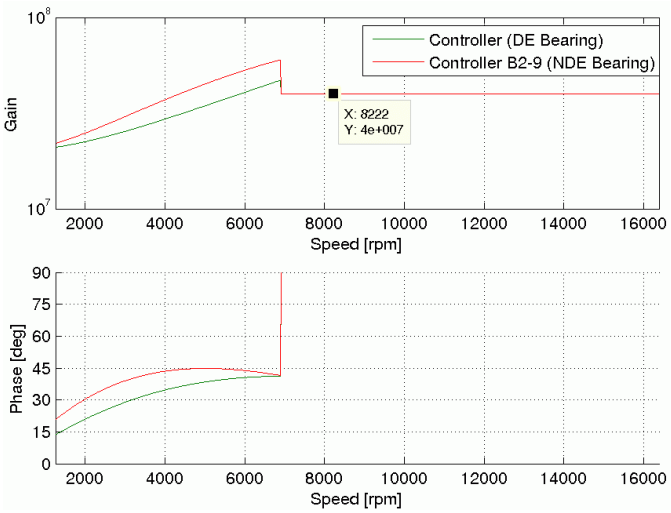

Figure 14. Synchronous transfer function

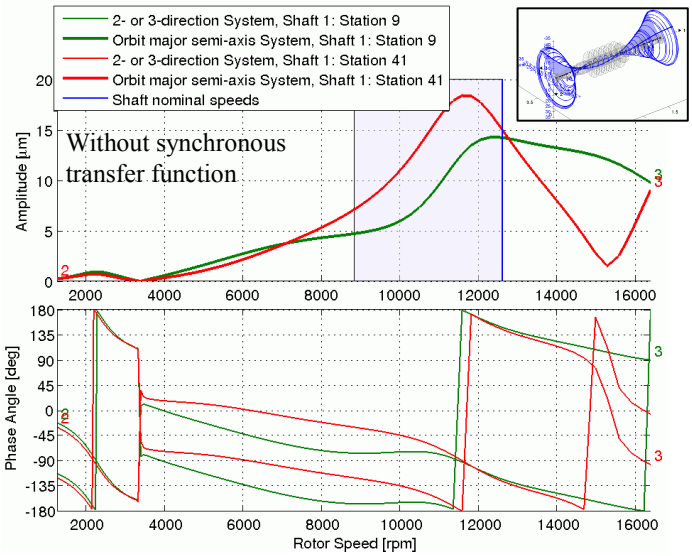

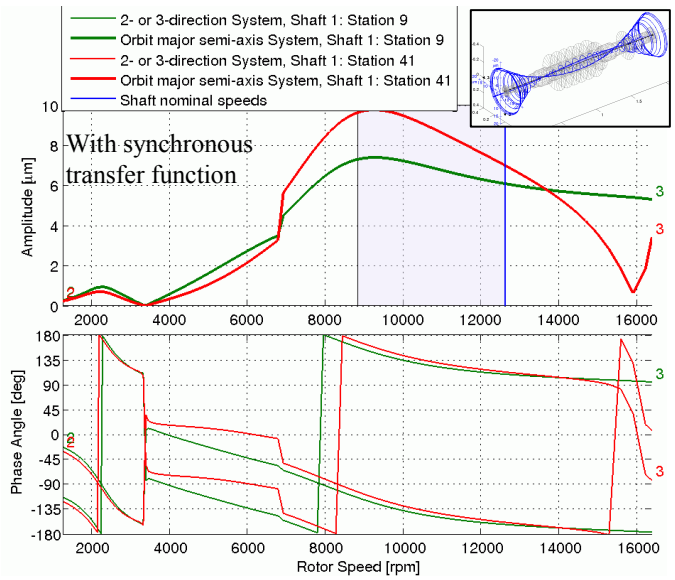

Figure 15. Sensor displacement response with and without synchronous characteristic

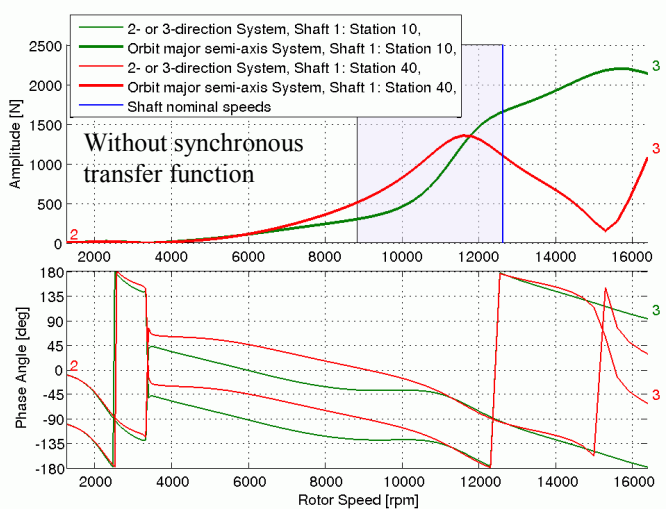

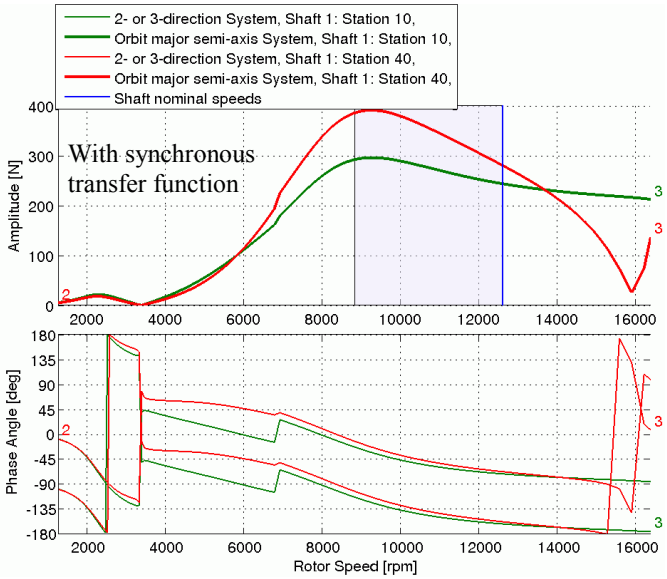

Figure 16. Bearing force response with and without synchronous characteristic

THE INFLUENCE OF THE BEARING SUPPORTS

The natural modes at nominal speed of the turbine generator train are shown in figure 17. The support displacement is indicated by the arrow at the bearing location. The shapes are shown in the same way as explained for figure 10.

The bending mode of the turbine in vertical direction at 68.1Hz turned out to be very sensitive to the bearing support characteristic. The static stiffness of the support is about one third of the oil film stiffness in the stiff vertical direction. The effective mass depends on the dynamic characteristic of the support. Different assumptions for the effective masses of the

turbine support on the generator side are summarized in table 1. Figure 17 is calculated with assumption 1, which was based on past experience.

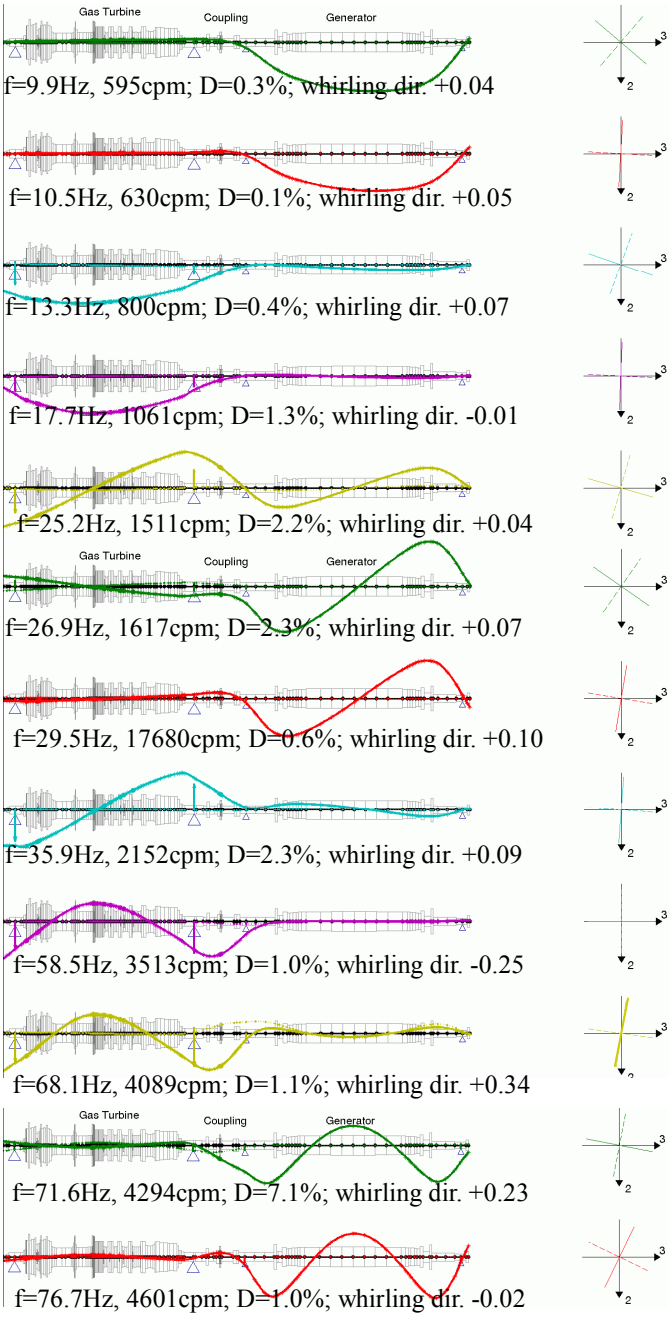

Figure 17. Natural modes at nominal speed

Table 1. Assumptions for the effective masses of the turbine bearing support on the generator side.

Assumption	1	2	3	4
Ratio of support to turbine rotor mass	9%	34%	0%	100%
Support natural frequency	71Hz	37Hz	infinite	22Hz

The assumption 2 in table 1 is derived from a 3D finite element model (FE model) of the support. The displacement force relation calculated from this model is shown in figure 18. The red line represents the characteristic of a one mass substitute model of the support. Assumptions 3 and 4 are extreme and not realistic. They were analyzed in order to get a better feeling for the overall behavior.

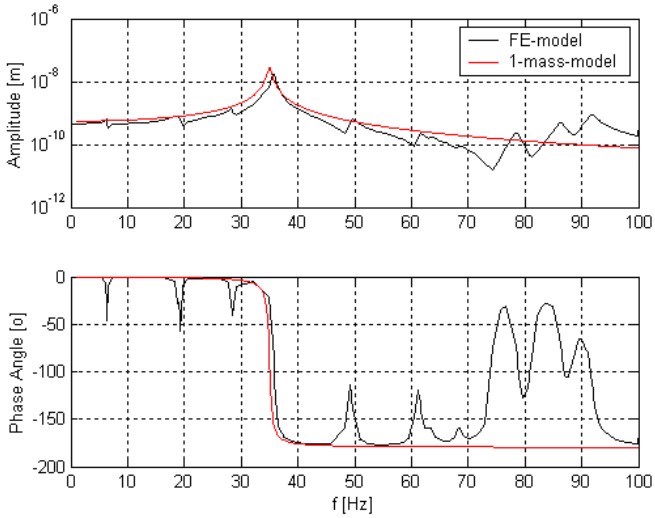

Figure 18. Support characteristic (displacement response per unit force excitation) of the turbine support on the generator side

The behavior of the turbine bending mode for different effective masses of the support is demonstrated in figure 19. It can be seen that with increasing mass ratio the deflection of the generator side turbine bearing decreases (large masses do not like to move) and the frequency drops considerably. Of course, other modes are also influenced by the mass ratio to some extent, especially the vertical tilting mode of the turbine, but not by such an amount, and they do not shift into the vicinity of the operating speed.

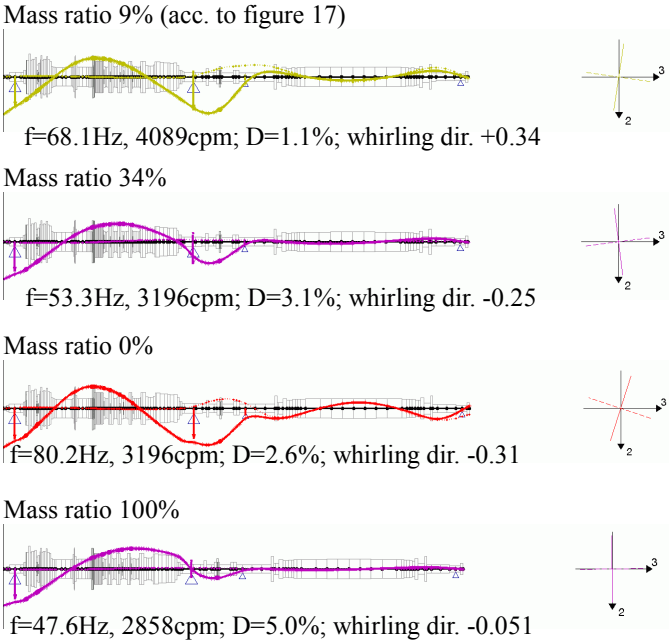

Figure 19. Turbine bending mode in vertical direction for different support characteristics

THE IMPACT OF SEAL FORCES

The tangential and radial seal forces of the labyrinths of the rotor in figure 3 for a circular unit shaft orbit are shown in figure 20. They are the forces from the seal on the rotor, i.e. positive tangential forces destabilize forward whirling modes and positive radial forces are in the same direction as the orbit radius, i.e. they bring the rotor out of center and thus soften the system.

The labyrinth seal forces were calculated with a Navier Stokes solver (see [17]). The tangential as well as radial force show a slight curvature caused by inertia effects. To include them in the model, mass coefficients are necessary. However, in the present case the effect is small.

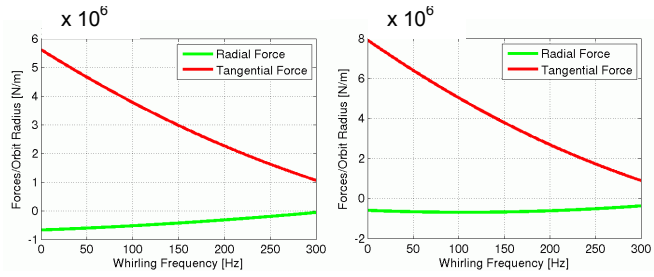

Figure 20. Radial and tangential labyrinth seal forces

The frequency at which the tangential force is zero, the so called swirl frequency, allows a rough assessment, which rotor modes are destabilized by the seals: Forward whirling modes with lower frequencies will be subjected to a damping reduction. For the labyrinth seals this frequency is beyond the shown frequency range to 300Hz.

The honeycomb seal forces in figure 21 for circular backward (neg. frequency) and forward (pos. frequency) orbits are strongly frequency dependent. They were calculated according to the method described in [10] and cannot be simply modeled by stiffness, damping and mass coefficients. They must be modeled by transfer functions in a similar way as magnetic bearings.

The swirl frequencies of the balance piston and interstage seal are around 50Hz and 70Hz, respectively.

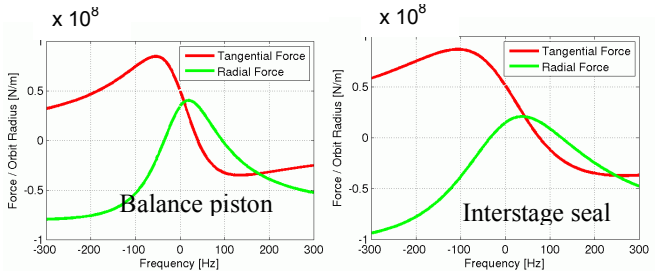

Figure 21. Rad. and tangential honeycomb seal forces

The eigenvalues of the system with and without the seals are shown in figure 22. The seals are considered in two steps for a better interpretation of the results. In a first step only the labyrinth seals are considered and in a second step all seals.

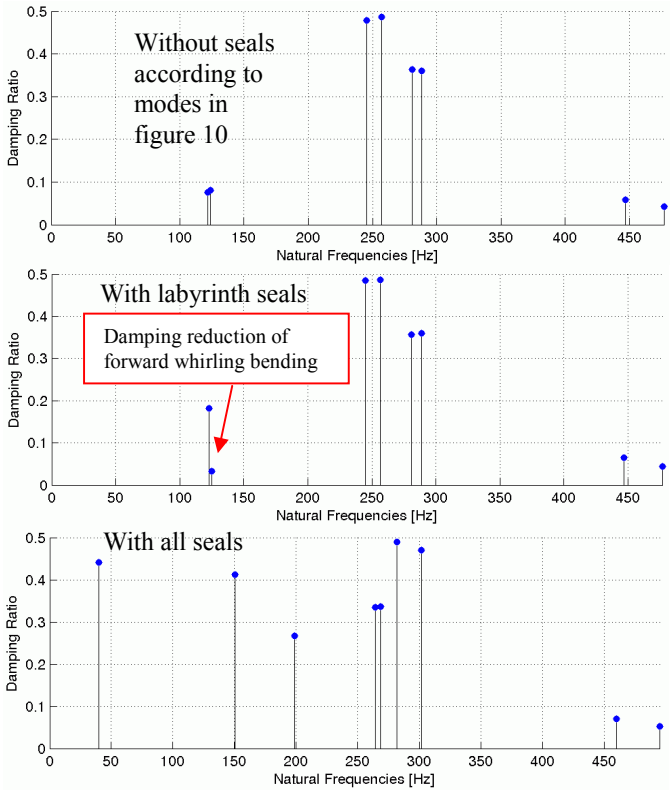

Figure 22. Eigenvalues with consideration of seal forces

The labyrinth seals mainly influence the forward and backward whirling first bending mode. The damping of the forward mode is decreased, of the backward mode increased. The other modes are almost not affected.

The impact of the honeycomb labyrinth seals is very big in a frequency range up to 300Hz. The second bending modes above 450Hz are only slightly influenced. The system with honeycomb seals is well damped. This is due to the large stiffening effect at higher frequencies (negative radial force) and the relatively low swirl frequency.

COUPLING OF TORSIONAL AND LATERAL VIBRATIONS IN GEARS

The coupling of lateral and torsional vibrations in gears is normally not considered. An additional coupling with axial vibrations can also occur. Lateral torsional coupling is of interest for the following reasons:

1. Due to the lateral vibration component the radial bearings can influence the damping of the torsional vibration modes. Normally they add damping, but they can also destabilize as shown for example in [18]. This reference also contains a comparison of measured and calculated stability thresholds, verifying this type of analysis.
2. Lateral excitations such as the unbalance can excite torsional vibrations and vice versa torsional excitations excite lateral vibrations. By means of a coupled model this can be simulated.
3. The natural vibration modes of a lateral torsional coupled model can be different from those of the decoupled systems.

In figure 23a and b the decoupled torsional and lateral vibration modes of pinion 1 of the gear compressor in figure 6 are compared to the corresponding modes of a coupled analysis of the complete gear compressor.

In the 3-dimensional plots of figure 23 the lateral vibrations are shown in blue, the torsional vibrations in red and the axial vibrations in green. The shape of the lateral vibrations is shown at two instants: The instant of maximum deflection, which corresponds to the line with the shaded area, and a quarter period later. Thus the whirling direction can be recognized. The torsional angles are plotted as transverse displacements in the vertical 2-direction. The angles are transformed to transverse displacements by the mesh radius of the respective shaft.

The comparison of the coupled and uncoupled analysis in figure 23 reveals that many bending modes of the pinion 1 do not deviate to a high extent. On the other hand there are some substantial changes. The bending mode in tooth contact direction at 419Hz does not appear in the coupled analysis. Instead a new mode with torsion of all three shafts appears at a frequency of 173Hz. The torsional mode of the pinion at 345Hz and 360Hz, respectively, is coupled to a lateral vibration in the coupled analysis, whose shape resembles the uncoupled mode at 419Hz. However, the frequencies do not deviate a lot. Thanks to the coupling the mode has a considerable damping of 4.7%.

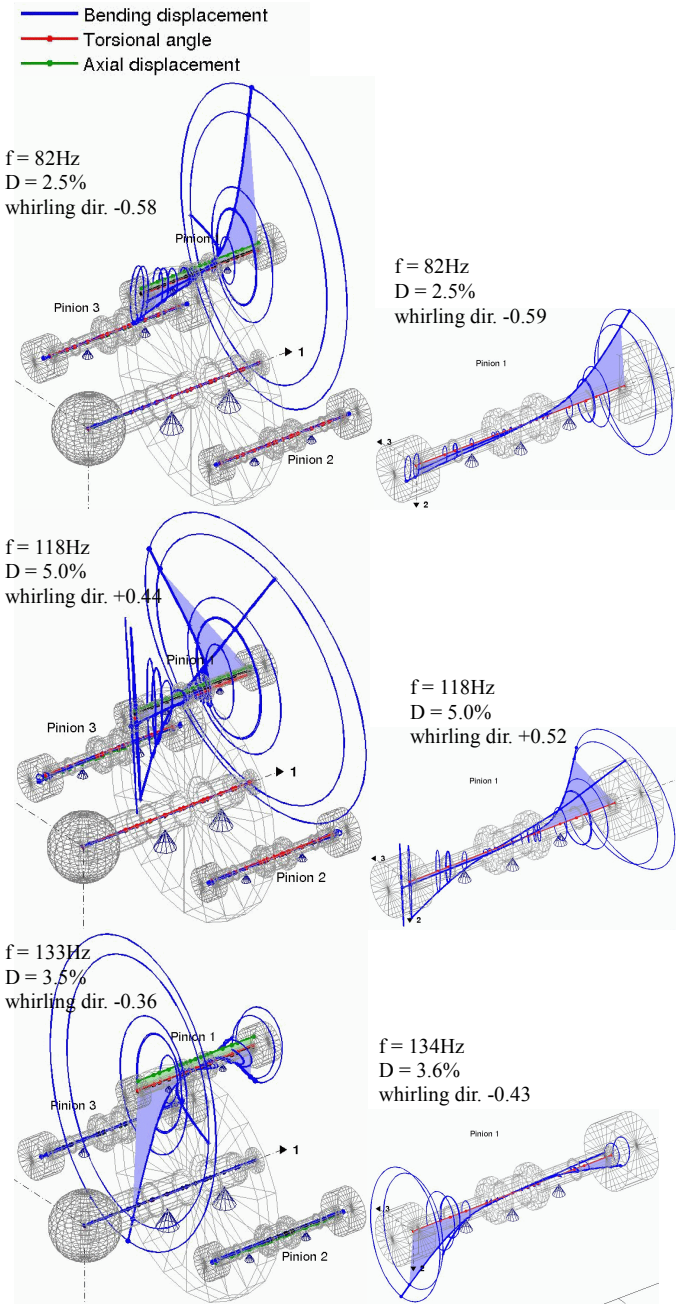

Figure 23a. Lateral and torsional modes of pinion 1, coupled and uncoupled

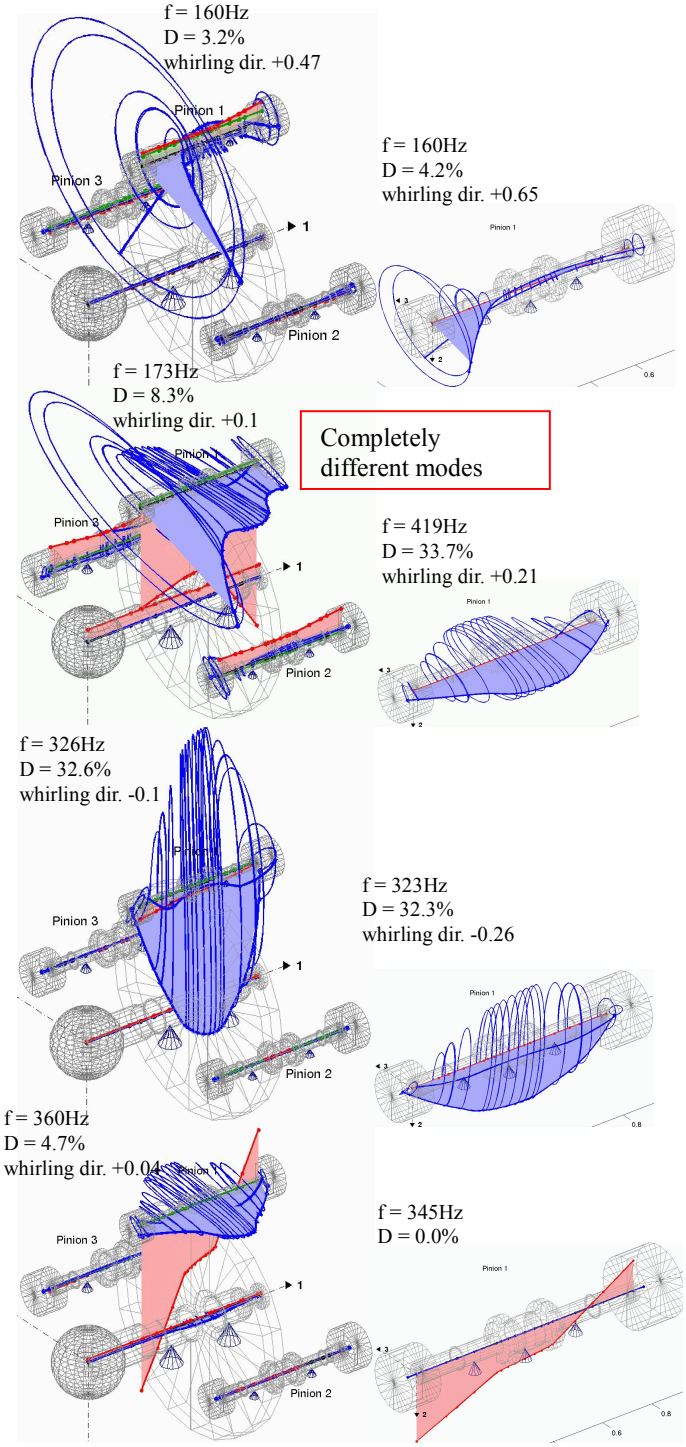

Figure 23b. Lateral and torsional modes of pinion 1, coupled and uncoupled

SUMMARY

The requirements of a modern tool for rotordynamic analyses are demonstrated for four examples, covering different types of bearings, the influence of bearing supports, seal forces acting on rotors and coupled vibrations as they can occur in gears.

Some of the requirements are new due to new technologies (e.g. magnetic bearings) or new research results (e.g. the frequency dependence of seal forces). In both cases the forces caused by rotor displacements are strongly frequency dependent and cannot be simply modeled by stiffness, damping and mass coefficients.

REFERENCES

1. Lund, J.; Thomsen, K.; 1978. “A Calculation Method and Data for the Dynamics of Oil Lubricated Journal Bearings in Fluid Film Bearings and Rotor Bearings System Design and Optimization”, ASME, New York (1978), pp. 1-28.
2. Nordmann, R.; 1974. “Ein Näherungsverfahren zur Berechnung der Eigenwerte und Eigenformen von Turborotoren mit Gleitlagern, Spalterregung, äusserer und innerer Dämpfung”, Dissertation Technische Hochschule Darmstadt.
3. Nelson, H. D.; McVaugh, J. M.; 1976. “The Dynamics of Rotor-Bearing Systems using Finite Element”, ASME Trans., Journal of Industry, Vol. 98(2), pp.593-600.
4. Gasch, R.; 1976. “Vibration of Large Turbo-Rotors in Fluid Film Bearings on an Elastic Foundation”, Journal of Sound and Vibration, Vol. 120, pp.175-182.
5. Nelson, H. D.; 1980. “A Finite Rotating Shaft Element using Timoshenko Beam Theory”, Trans. ASME, Journal of Mechanical Design, Vol. 102(4), pp.793-803.
6. Mittwollen, N.; Glienicke, J.; 1990. “Operating Conditions of Multi-Lobe Journal Bearings Under High Thermal Loads”, ASME Journal of Tribology, Vol. 112, April 1990.
7. Spirig, M.; Schmied, J.; Jenckel, P.; Kanne, U.; 2002. “Three Practical Examples of Magnetic Bearing Control Design Using a Modern Tool”, ASME Journal of Engineering for Gas Turbines and Power, October 2002, Vol. 124, pp. 1025-1031.
8. Nordmann, R.; Dietzen, F. J.; 1987. “Calculating Rotor-dynamic Coefficients of Seals by Finite-Difference Techniques”, ASME Journal of Tribology, July 1987, Vol. 109, pp. 388-394.
9. Childs, D.; 1993. “Turbomachinery Rotordynamics”, Wiley Inter Science, 1993.
10. Kleynhans, G. F.; Childs, D. W.; 1996. “The Acoustic Influence of Cell Depth on the Rotordynamic Characteristics of Smooth Rotor / Honeycomb-Stator Annular Gas Seals” ASME paper No. 96-GT-122, presented at the ASME Turbo Expo, Birmingham, UK, 1996.

11. Grigoriev, B.; Schmied, J.; Fedorov, A.; Lupuleac, S.; 2006. “Consideration of the Pressure Entrance Loss for the Analysis of Rotordynamic Gas Seal Forces”, Paper-ID 245, 7th IFTOMM Conference on Rotor Dynamics, Vienna, Austria, 25-28 September 2006.
12. API (American Petroleum Institute) Standard 617, 7th Edition July 2002.
13. MADYN 2000, Version 2.0, Documentation 2006.
14. Klement, H. D.; 1993. “Berechnung der Eigenfrequenz und Stabilität von Rotoren mit MADYN“, VDI Bericht Nr. 1082.
15. Mittwollen, N.; 1987. “Taschenlager-Optimierung”, FVV-Bericht Vorhaben Nr.339.
16. Schmied J.; Nijhuis A.B.M.; Shultz R. R.; 1999. “Rotordynamic Design Considerations for the 23MW NAM-GLT Compressor with Magnetic Bearings", ImechE Fluid Machinery Symposium, The Hague.
17. Weiser, H. P.; 1989. “Ein Beitrag zur Berechnung der dynamischen Koeffizienten von Labyrinthdichtungs-systemen bei turbulenter Durchströmung mit kompressiblen Medien“, Dissertation TU Kaiserslautern.
18. Viggiano, F.; Schmied J.; 1996. “Torsional Instability of a geared compressor shaft train”, IMechE paper C508/013.